Smart Structures and Systems, *Vol. 28, No. 4 (2021) 553-566*
https://doi.org/10.12989/sss.2021.28.4.553

Hybrid fragility curve derivation of buildings based on post-earthquake reconnaissance data

Sangmok Lee [1a], Do-Soo Moon [2b], Byungmin Kim [1c], Jeongseob Kim [1d] and Young-Joo Lee*[1]

[1] *Department of Urban and Environmental Engineering, Ulsan National Institute of Science and Technology (UNIST), Ulsan 44919, Republic of Korea*
[2] *Department of Civil Engineering, University of Hawaii at Manoa, HI 96822, USA*

(*Received January 8, 2021, Revised May 18, 2021, Accepted May 28, 2021*)

Abstract. This study proposes a new hybrid method that uses both of post-earthquake reconnaissance data and numerical analysis results based on a finite element (FE) model. As the uncertainty of a capacity threshold for a structural damage state needs to be estimated carefully, in the proposed method, the probabilistic distribution parameters of capacity thresholds are evaluated based on post-earthquake reconnaissance data. Subsequently, the hybrid fragility curves were derived for several damage states using the updated distribution parameters of capacity thresholds. To illustrate the detailed process of the proposed hybrid method, it was applied to piloti-type reinforce concrete (RC) buildings which were affected by the 2017 Pohang earthquake, Korea. In the example, analytical fragility curves were derived first, and then hybrid fragility curves were obtained using the distribution parameters of capacity thresholds which were updated based on actual post-earthquake reconnaissance data about the Pohang city. The results showed that the seismic fragility estimates approached to the empirical failure probability at 0.27 g PGA, corresponding to the ground motion intensity of the Pohang earthquake. To verify the proposed method, hybrid fragility curves were derived with the hypothetical reconnaissance data sets created based on assumed distribution parameters with errors of 10% and 1%. As a result, it was identified that the distribution parameters accurately converged to the assumed parameters and the case of 1% error had better convergence than that of 10% error.

Keywords: capacity threshold; hybrid curve; piloti-type buildings; post-earthquake reconnaissance; seismic fragility

1. Introduction

An earthquake is one of the most devastating natural disasters which can cause an enormous amount of structural damages, economic losses, and casualties. Risk assessment is essential to mitigate and manage such seismic hazard, and fragility curves have been recognized as a key component of seismic risk analysis (Yoon *et al*. 2018). For example, software packages of seismic risk assessment such as HAZUS (FEMA 2013) and Ergo-EQ (Steelman *et al*. 2007) estimate post-earthquake losses using seismic fragility curves of various infrastructures. As the loss estimates are directly used for decision-makers to set up mitigation plans to alleviate the disastrous impact of earthquakes (Kircher *et al*. 2006), the derivation of accurate seismic fragility curves is crucial for effective seismic risk assessment and mitigation.

Seismic fragility curves represent the relationship between earthquake ground motion intensity and probability of exceeding certain damage levels, which have been broadly used for describing fragility analysis results of various structures (Liu and Zhang 2017, Li *et al*. 2018, Moradloo *et al*. 2018, Razzaghi *et al*. 2018). Four different types of fragility curves are known to be available based on how to derive them, namely empirical, judgmental, analytical, and hybrid methods (Rossetto and Elnashai 2003). Empirical (Rosti *et al*. 2020, Giordano *et al*. 2021), judgmental (Mosleh and Apostolakis 1986, Jaiswal *et al*. 2012), and analytical fragility curves (Silva *et al*. 2014, Martínez *et al*. 2017) can be obtained from actual damage data, expert opinions, and numerical simulations with analytical models, respectively, but they have their own strengths and weaknesses. Empirical fragility curves would be the most realistic, but it is hard to acquire enough structural damage field data. Judgmental curves can be easily derived on the basis of expert opinions, but they would be highly subjective depending on the experience and judgement of the selected expert team. Analytical fragility curves are most widely used as they can be numerically developed for a variety of structural systems with their representative analytical models employing different simulation approaches, but the derived fragility curves may be not that accurate with the choice of simulation models and techniques (Rossetto and Elnashai 2003).

To compensate the shortcomings of empirical, judgmental, or analytical fragility curves, hybrid fragility curves can be developed by means of different

*Corresponding author, Associate Professor,
E-mail: ylee@unist.ac.kr
[a] Ph.D., E-mail: smlee@unist.ac.kr
[b] Assistant Professor, E-mail: dsmoon@hawaii.edu
[c] Associate Professor, E-mail: byungmin.kim@unist.ac.kr
[d] Associate Professor, E-mail: jskim14@unist.ac.kr

ISSN: 1738-1584 (Print), 1738-1991 (Online)

combinations of at least two types of data (Pitilakis *et al*. 2014). For instance, empirical data is frequently used in combination with numerical analysis results from structural analysis models (e.g., FE models) to get more realistic fragility curves. However, the derivation of these hybrid fragility curves is still a challenging task because it is not always possible to collect sufficient field damage information and how to integrate lacking empirical data with an FE analysis effectively is always in question. Furthermore, the derivation of a hybrid seismic fragility curve may require solving an optimization problem with repetitive seismic fragility analysis, which can be computationally expensive. Owing to these difficulties, few studies have attempted to derive hybrid fragility curves. Singhal and Kiremidjian (1998) conducted hybrid fragility assessment of RC buildings located in earthquake-prone areas. Park and Ang (1985) selected a damage index to quantify the level of building damage, and empirical data were used to adjust lognormal distribution parameters of the median damage index through Bayesian updating. In their studies, failure probabilities were initially estimated using analytical building models; subsequently, the obtained analytical probabilities were modified with the updated median damage index. The update was performed at six ground motion intensities where the empirical data were available. They adopted Monte Carlo simulation (MCS), which is a sampling-based method, to calculate failure probabilities. Another hybrid fragility study was conducted by Kappos *et al*. (2006). They investigated seismic fragility assessment of RC and unreinforced masonry structures. A loss index, proposed by Kappos *et al*. (1998), was scaled by the ratio of the actual loss (estimated from empirical data collected at a single ground motion intensity) to the analytical loss (computed from structural analysis results). Then, the ratio was equally applied to alter loss indices for all damage states with varying ground motion intensities. They adopted a simple mathematical form to derive their seismic fragility curves.

In fragility analysis where seismic supply (or capacity) from a structure and seismic demand from earthquakes are compared, there is a need to pay a special attention to seismic capacity thresholds of the given structure since the uncertainty in threshold values may differ depending on damage level states, the so-called limit states. The capacity threshold often has considerable uncertainty as it is associated with many structural parameters. Accordingly, the selection of capacity thresholds should be carefully considered for defined limit states. Deterministic capacity thresholds have been implemented in many studies (Kwon and Elnashai 2006, Güneyisi and Altay 2008, Ji *et al*. 2009, Moon *et al*. 2018). Alternatively, the uncertainty of capacity thresholds has been assumed based on engineering experience and judgment in some cases (Wen *et al*. 2004, Ramamoorthy *et al*. 2006, Hueste and Bai 2007, Ellingwood *et al*. 2007). Yu *et al*. (2016) studied the capacity uncertainty for RC frame structures. Considering structural parameters, such as material properties and gravity loads, as random variables, they generated random samples and performed nonlinear pushover analyses using the generated samples. The results indicated that the extent of capacity uncertainty varied depending on damage states, and it tended to increase as the damage state level risen. A similar trend of capacity uncertainty variation can be found in the study by Dolšek (2012). The seismic risk of an RC building was assessed considering various uncertainties in structural parameters and ground motions. Incremental dynamic analyses (Vamvatsikos and Cornell 2002) were performed with given ground motions and structural parameters to evaluate the median and logarithmic standard deviation values of selected limit states. It was identified that the logarithmic standard deviation values increased with the severity of limit states. Montiel and Ruiz (2007) explored the influence of structural capacity uncertainty on seismic reliability of three RC buildings. They analyzed lognormal distribution parameters of the structural capacity in the yielding drift and near-collapse limit states. The results showed that the logarithmic standard deviation of the yielding drift limit state was smaller than that of the near-collapse limit state. In addition, the logarithmic standard deviation varied with structures; thus, the structural capacity uncertainty should be prudently determined depending on structural types as well as limit states.

To overcome the limitations of previous studies on seismic fragility analysis and derive more realistic seismic fragility curves using empirical and analytical data, this study proposes a new hybrid method which consists of four steps: 1) the derivation of analytical fragility curves; 2) the identification of probabilistic distribution parameters of capacity thresholds through optimization; 3) the updates of the distribution parameters using the Bayesian updating; and 4) the derivation of hybrid fragility curves with the updated distribution parameters. In the proposed method, the distribution parameters of capacity thresholds are identified more carefully, based on the empirical fragility estimates obtained from post-earthquake reconnaissance data because the uncertainty of a capacity threshold may vary depending on damage states as mentioned above. To find out distribution parameters of capacity thresholds and derive hybrid fragility curves using the acquired parameters efficiently, in the proposed method, an efficient computational platform of seismic fragility analysis is also introduced. The proposed hybrid method can be applied to any types of structural systems when empirical data are available, and more detailed explanations of the proposed method and its application are presented in the subsequent sections.

2. Proposed method for deriving hybrid fragility curves

2.1 Introduction of efficient computational platform

As aforementioned, the proposed method in this study tries to determine the probabilistic distribution parameters of capacity thresholds for various damage states. Mathematically, this is an optimization problem, and it requires performing seismic fragility analyses repetitively to obtain various distribution parameters of capacity thresholds. A seismic fragility curve is a probabilistic

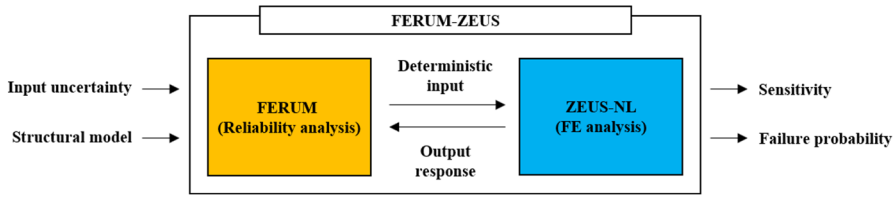

Fig. 1 Data flow in FERUM-ZEUS (Lee and Moon 2014)

indicator of structural safety against earthquakes, which presents failure probabilities at various ground motion intensities; there are two different approaches available to derive the curve (Lee and Moon 2014, Moon *et al*. 2018): sampling-based methods such as MCS and non-sampling-based methods such as the first order reliability method (FORM) (Der Kiureghian 2005). Sampling-based methods have been used extensively because they are conceptually straightforward. However, these methods are often costly because they commonly require a large number of structural analyses for reliable fragility estimates. On the other hand, the FORM is one of the representative non-sampling-based methods for reliability analysis (Der Kiureghian 2005) and it has been widely used to compute failure probabilities of a given limit-state function in several previous studies due to its computational efficiency (Lee and Song 2012, Lee and Moon 2014, Lee *et al*. 2016, Moon *et al*. 2018). In reliability analysis, a limit-state function defines a failure criterion and it is expressed by either random or deterministic variables. The FORM performs iterative computation to estimate a failure probability when variable uncertainties are considered. If structural model parameters are selected as random variables to consider uncertainty, repeated structural analyses are required in the FORM.

An efficient computational platform was recently developed to handle repetitive structural analyses needed in the FORM (Lee and Moon 2014, Kim *et al*. 2017). This computational platform, referred to as FERUM-ZEUS, links two software packages, FERUM and ZEUS-NL. FERUM is a reliability analysis software package developed by the University of California, Berkeley, and it provides a variety of reliability methods, including the FORM (Haukaas 2003, Lee *et al*. 2008). ZEUS-NL is a fiber element-based nonlinear finite element analysis program developed by the Mid-America Earthquake Center (Elnashai *et al*. 2010), and it is an advanced structural analysis tool specialized for earthquake engineering simulation applications (Lee and Moon 2014). Fig. 1 shows the overall data flow in the FERUM-ZEUS computational platform. Under the established platform, repeating structural analysis can reflect the uncertainty in structural model parameters, and input and output data for reliability or structural analysis can be exchanged automatically, which enables cost-efficient computation using FORM. Lee and Moon (2014) and Moon *et al*. (2018) proved the cost efficiency of their proposed FERUM-ZEUS framework by comparing it with the MCS under the same numerical simulation, and its application was also demonstrated by deriving seismic fragility curves of space RC frame structures with plan irregularities (Moon *et al*. 2018). This study employs the FERUM-ZEUS platform to determine probabilistic

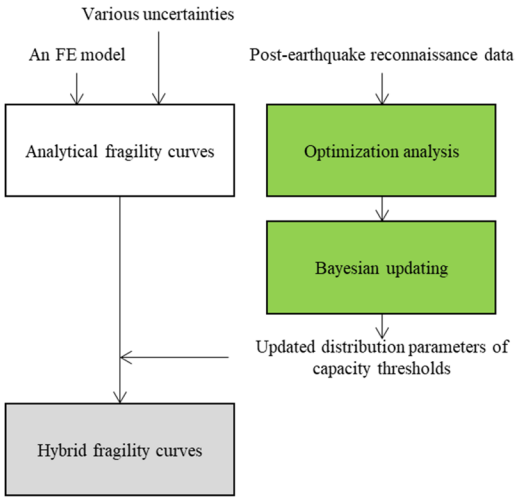

Fig. 2 Framework of the proposed hybrid method

distribution parameters of capacity thresholds and to develop seismic fragility curves based on the parameters efficiently.

2.2 Proposed hybrid method

This study proposes a new hybrid method combining empirical and analytical methods of fragility analysis, which can compensate for the deficiency of analytical models and the insufficiency of empirical data. Particularly, empirical data is utilized to estimate probabilistic distribution parameters of capacity thresholds that best describe the empirical failure probability in a target area; thus, it contributes to derive more accurate and realistic fragility curves. Four steps are identified to derive hybrid fragility curves using the proposed method, and Fig. 2 presents the overall framework.

The first step in the proposed method is the derivation of analytical fragility curves using FERUM-ZEUS. In this step, a representative FE model is constructed, and the distribution parameters of capacity thresholds are assumed identically for all selected damage states (Wen *et al*. 2004). The assumed distribution parameters of the capacity thresholds are considered as prior parameters. The second step starts from the collection of post-earthquake reconnaissance data in the target area. From the post-earthquake reconnaissance data, the empirical failure probabilities, which can be defined as the ratio of the number of buildings that belong to or exceed a given damage state to the total number of buildings in the interested area (Askan and Yucemen 2010), are evaluated for each damage state. Subsequently, the distribution

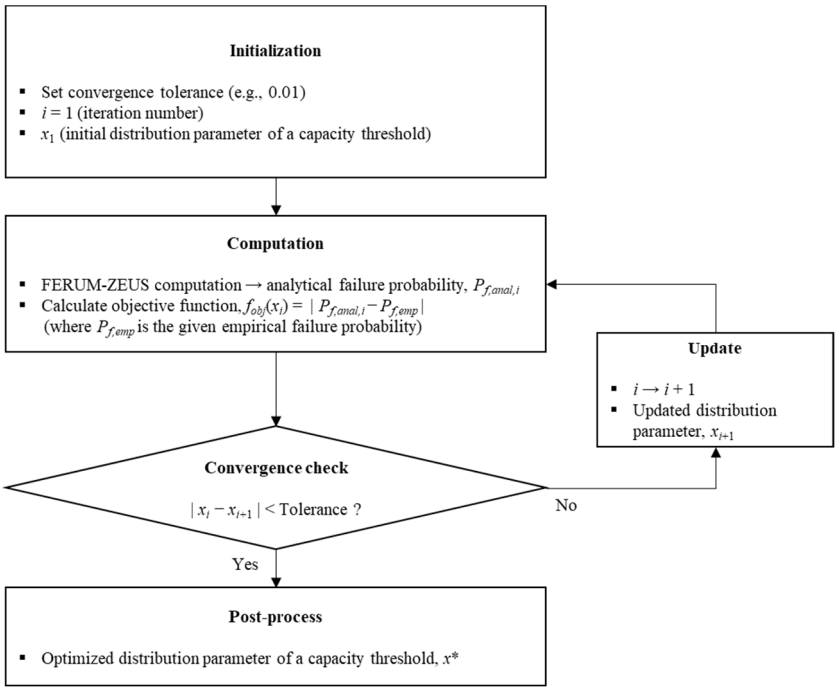

Fig. 3 Flowchart for optimization analysis

parameter of the capacity threshold optimized to the empirical failure probability is computed. To accomplish this, an optimization algorithm in MATLAB is linked to the code of FERUM-ZEUS. Fig. 3 shows the flowchart of the optimization analysis.

The optimization analysis is conducted with repetitive fragility analyses to find a solution for minimizing a given objective function; FERUM-ZEUS works continuously to compute failure probabilities at every iteration in the optimization analysis. The optimization problem is expressed by the following equation

$$x^* = \text{argmin}\{f_{obj}(x)\} \quad (1)$$

where "argmin" represents the argument of the minimum of the objective function ($f_{obj}(x)$) that denotes the absolute difference between the empirical failure probability and analytical failure probability, and x^* is the optimized distribution parameter of a capacity threshold. Once the optimized distribution parameter is determined, it is considered as the likelihood observed in the target area.

In the third step, the initially assumed distribution parameter of the capacity threshold (i.e., prior) is updated with the optimized parameter (i.e., likelihood) through Bayesian updating (Ang and Tang 2007). The following equation presents the formula for Bayesian updating for the parameter x

$$f''(x) = kL(x)f'(x) \quad (2)$$

where $f'(x)$ is the prior distribution, $L(x)$ is the likelihood function, $f''(x)$ is the posterior distribution of x, and $k = \left[\int_{-\infty}^{\infty} L(x)f'(x)dx\right]^{-1}$ is the normalizing constant. This is also called the Bayesian parameter estimation, and the more details can be found in a study of Ang and Tang (2007). In this study, the probabilistic distribution of x is assumed to be lognormal. The updated distribution parameter of a capacity threshold denotes the posterior, and it is applied to derive the hybrid fragility curves using FERUM-ZEUS, which is the last step of the proposed method.

3. Illustrative example

3.1 FE model construction

To illustrate the proposed method, it is applied to the seismic fragility analysis of piloti-type RC buildings in South Korea. On November 15, 2017, an earthquake with a local magnitude (M_L) of 5.4 hit the southeastern Korean Peninsula. Many structures were subjected to this earthquake, and several piloti-type RC buildings, in particular, were severely damaged (Kang *et al*. 2019, Kim *et al*. 2020a). Accordingly, this study focuses on the structural damage and seismic fragility of piloti-type RC buildings.

For the seismic analysis using the proposed method, an FE model is constructed in ZEUS-NL. The FE model is benchmarked from a previous study (Kim *et al*. 2018), and it represents a typical mid-story piloti-type RC building that can be often found in the actual damaged area; it consists of a moment frame in the first story and a structural wall system in the upper stories. The height of the first story is 3.2 m, while other stories is 3.0 m in height. The first story includes thirteen columns supporting the upper stories that are composed of structural walls, and there is a staircase in the middle of one side. Fig. 4 shows the plan view of the first story and the created FE model. All columns have the same cross-section (400 mm × 600 mm) with sixteen D19

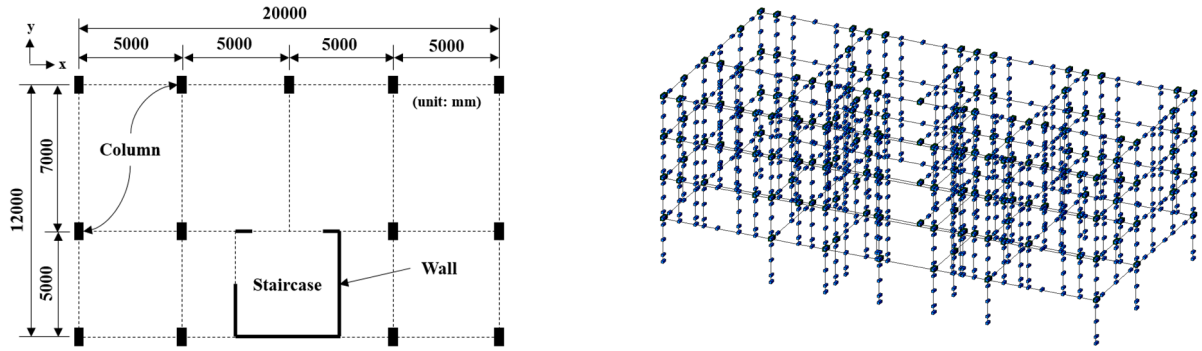

(a) Plan view of the first story (b) FE model constructed for ZEUS-NL

Fig. 4 Plan view of the first story and the FE model constructed for ZEUS-NL

(a) Concrete (b) Steel

Fig. 5 Stress-strain curves

Table 1 Dead and live loads in the FE model

Section	Dead load (kN/m^2)	Live load (kN/m^2)
Typical	5.2	2.0
Staircase	2.0	2.0
Rooftop	5.0	1.0

reinforcing steel bars. The walls have a thickness of 180 mm with vertical reinforcing steel (D10@300). The compressive strength of concrete and the yielding strength of reinforcing steel are defined as 21 MPa and 400 MPa, respectively. Material nonlinear behaviors for both concrete and steel, as shown in Fig. 5, are considered in FE analysis. The gravity load is assumed to be 1.0DL + 0.25LL, where DL and LL denote the dead and live loads, respectively. Table 1 presents the gravity load information defined in the analytical model. The natural period of the first mode of the ZEUS-NL model was found to be 0.251 second.

3.2 Definition of damage states and uncertainties

Three damage states are considered, which are light, moderate, and severe damage states. To define capacity thresholds for the three damage states quantitatively, a conventional nonlinear pushover analysis was performed using inverted-triangle load, and inter-story drift (ISD) ratio was selected as the engineering demand parameter. Because the first story of the piloti-type analytical model is weaker in terms of the lateral force resistance or more flexible than

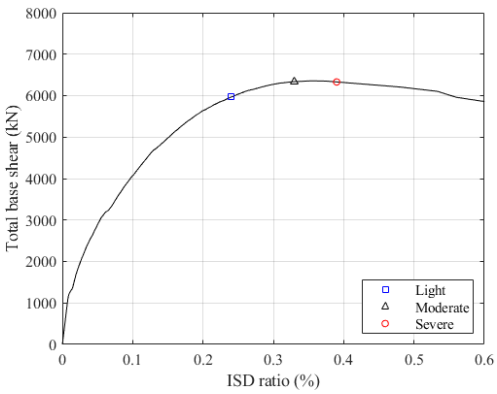

Fig. 6 Nonlinear pushover curve with ISD thresholds

the upper stories, this study focuses on ISD responses of the first story (or soft story). In fact, it was observed that first stories of many piloti-type RC buildings were significantly affected by the 2017 Pohang earthquake (Sim *et al*. 2018). From the adaptive pushover analysis, a nonlinear pushover curve of total base shear versus first-story ISD ratio was obtained as shown in Fig. 6.

Based on the pushover curve, the capacity thresholds for the three damage states were determined, as presented in Table 2. The capacity threshold for light damage was defined at the first yielding of reinforcing steel in any column members, and that for moderate damage was determined at the maximum element strength in the column members, as suggested in previous studies (Kwon and

Table 2 ISD thresholds for three damage states

Damage state	ISD ratio (%)
Light	0.24
Moderate	0.33
Severe	0.39

Elnashai 2006, Moon *et al*. 2018). The capacity threshold for severe damage was defined at the point where confined concrete reached about 15 percent strength degradation beyond the peak point on the pushover curve (Lee *et al*. 2018).

Uncertainties inherent in material properties, capacity thresholds, and earthquake ground motions were considered, and the material properties and capacity thresholds were introduced as random variables in the FORM analysis to consider their uncertainty. All random variables were assumed to follow lognormal distributions, and Table 3 gives the lognormal distribution parameters of the selected random variables. In the table, λ and ζ denote the logarithmic mean and logarithmic standard deviation, respectively. The coefficients of variation (c.o.v.s) of the random variables were determined according to previous studies (Barbato *et al*. 2010, Paik *et al*. 2011). The mean values of capacity thresholds for three damage states were estimated from the nonlinear pushover analysis, as mentioned above, and their logarithmic standard deviations were assumed to be the same for all three damage states (Wen *et al*. 2004). The proposed hybrid method can be applied to determine both of the logarithmic mean and the logarithmic standard deviation of a capacity threshold if sufficient amount of post-earthquake reconnaissance data is available. However, only one set of data is available in this illustrative example, so the c.o.v. was chosen as the target distribution parameter in the following analysis. The initially assumed c.o.v. of the capacity threshold is considered as the prior c.o.v., and it is used to derive analytical fragility curves. Then, the prior c.o.v. of the capacity threshold is updated based on the post-earthquake reconnaissance data as described in Section 2.2, and the updated c.o.v. (i.e., posterior c.o.v.) value is applied for hybrid fragility assessment.

To consider the uncertainty of earthquake ground motions, seven input ground motions recorded at the Pohang Seismological Observatory are used for the nonlinear time-history analysis. The input earthquake records were obtained from the National Earthquake Comprehensive Information System database, which is operated by the Korea Meteorological Administration. The peak ground acceleration (PGA) was adopted as the ground motion intensity measure. Table 4 shows the information related to the selected earthquake ground motions, and Fig. 7 shows the acceleration time-history records of the input ground motions. Both translational components (i.e., East-West (EW) and North-South (NS)) of the input motions were applied simultaneously in nonlinear time-history analysis. The original ground records were scaled up and down in order to ensure that a broad range of ground motion intensities were included. In addition, the damping ratio of the structural model was considered as 5% in the nonlinear time-history analysis.

3.3 Derivation of analytical fragility curves

As the first step of the proposed method, analytical fragility curves of the studied structure were derived with FERUM-ZEUS. The FORM was used to calculate failure probabilities for a given limit-state function ($g(\mathbf{x})$). The limit-state condition of the structural damage state is assumed to be achieved when the maximum ISD demand values of any first-story column members reaches to the specified ISD threshold; thus, the limit-state function, $g(\mathbf{x})$, is defined as follows

$$g(\boldsymbol{x}) = \mathrm{ISD}_{\mathrm{DS}} - max\begin{bmatrix}\mathrm{ISD}_{\mathrm{C01}}(\boldsymbol{x}), & \mathrm{ISD}_{\mathrm{C02}}(\boldsymbol{x}),\cdots,\\ \mathrm{ISD}_{\mathrm{C13}}(\boldsymbol{x})\end{bmatrix} \quad (3)$$

where $\mathrm{ISD}_{\mathrm{DS}}$ is the ISD threshold value for each damage

Table 4 Selected earthquake ground motions

No.	Date	M_L	PGA (g) of EW	PGA (g) of NS
1	09/12/2016	5.8	0.0284	0.0261
2	11/15/2017	5.4	0.2441	0.2726
3	09/12/2016	5.1	0.0127	0.0106
4	07/05/2016	5.0	0.0023	0.0025
5	09/19/2016	4.5	0.0051	0.0056
6	11/15/2017	4.3	0.0453	0.0688
7	09/25/2014	3.8	0.0001	0.0001

Table 3 Lognormal distribution parameters of random variables (Barbato *et al*. 2010, Paik *et al*. 2011, Wen *et al*. 2004)

Random variable	Distribution type	Mean	c.o.v.	λ	ζ
Concrete compressive strength	Lognormal	21 MPa	0.0630	3.0425	0.0629
Concrete strain at compressive strength	Lognormal	0.002	0.2000	−6.2342	0.1980
Steel yield strength	Lognormal	400 MPa	0.1000	5.9865	0.0998
Elastic modulus	Lognormal	200,000 MPa	0.0330	12.2055	0.0330
ISD threshold for light damage	Lognormal	0.0024	0.3070	−6.0773	0.3000
ISD threshold for moderate damage	Lognormal	0.0033	0.3070	−5.7588	0.3000
ISD threshold for severe damage	Lognormal	0.0039	0.3070	−5.5918	0.3000

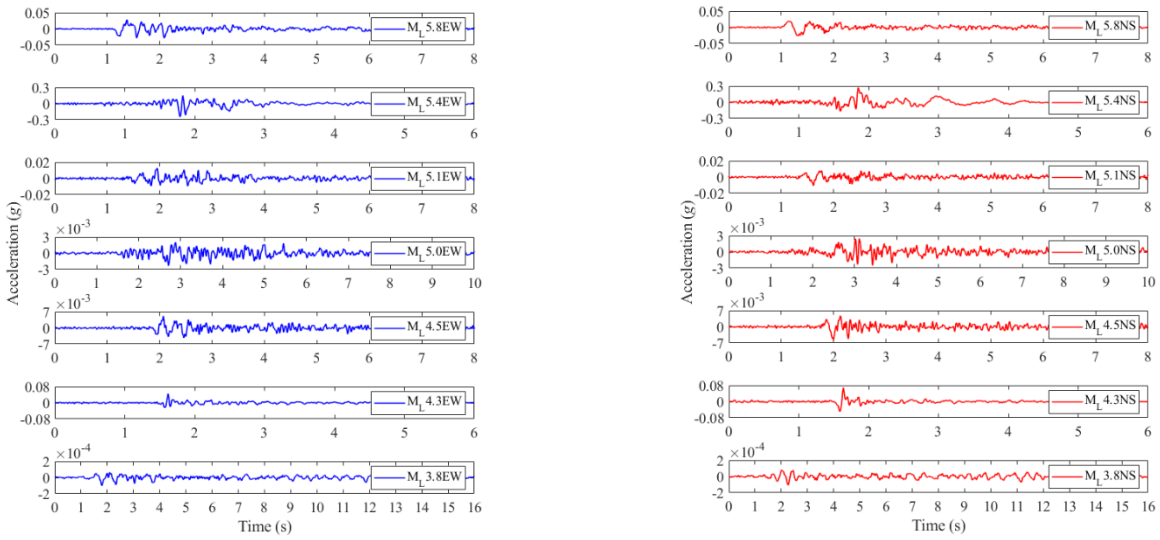

(a) Light damage (b) Moderate damage

Fig. 7 Acceleration time history records of the selected input ground motions

state presented in Table 2; ISD_{C01}, ISD_{C02}, …, ISD_{C13} denote the ISD demand values of the thirteen columns (C01–C13) on the first story; and **x** is the vector of random variables which are presented in Table 3.

Fig. 8 depicts analytical fragility curves obtained using the FERUM-ZEUS platform about the studied piloti-type structure for different damage limit states. The fragility curves were plotted with the seven input ground motions; furthermore, the average fragility curves representing mean failure probabilities over all input motions at each ground motion intensity were plotted. As expected, the failure probabilities decreased as the level of damage states moved from light to severe damage. The structural responses varied considerably along with the input ground motions, as shown in the figures. If seismic fragility curves are derived only using certain input ground motion, they can produce

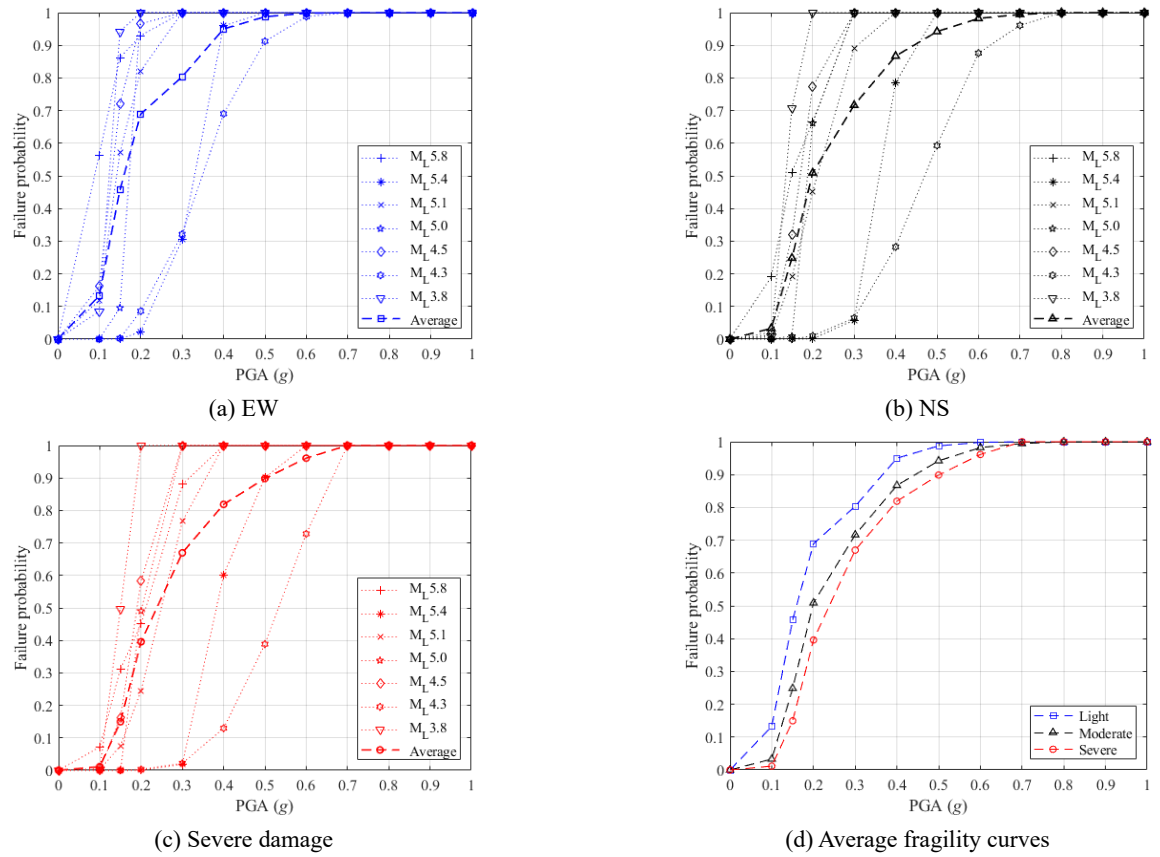

(a) EW (b) NS

(c) Severe damage (d) Average fragility curves

Fig. 8 Analytical fragility curves

Table 5 Average failure probabilities of the analytical fragility curves for each damage state

Damage state	PGA (g)										
	0.1	0.15	0.2	0.3	0.4	0.5	0.6	0.7	0.8	0.9	1.0
Light	0.133	0.457	0.689	0.804	0.950	0.987	0.998	1	1	1	1
Moderate	0.033	0.248	0.509	0.716	0.867	0.942	0.982	0.994	1	1	1
Severe	0.012	0.150	0.396	0.670	0.819	0.899	0.961	1	1	1	1

biased outcomes. Hence, the average curves are more reasonable representations of seismic vulnerability of the structures in the target area. Table 5 summarizes the average failure probabilities of derived seismic fragility curves with varying ground motion intensities for each damage state.

3.4 Post-earthquake reconnaissance data

As aforementioned, reconnaissance data about actual damaged structures can be valuable resources for understanding the seismic fragility of structures in a target area. Many structures were affected and damaged during the 2017 Pohang earthquake of magnitude 5.4; among them a number of piloti-type RC buildings located in the northern Pohang city were significantly damaged. Fig. 9 shows the epicenter of the Pohang earthquake with the location of the target area where piloti-type RC buildings are densely distributed. The epicentral distance from the earthquake source to the target area was approximately 3.8 km. To collect damaged building data, post-earthquake reconnaissance was intensively performed with the lead of American Concrete Institute (ACI) from December 8 to 13, 2017 (Sim *et al*. 2018). The reconnaissance group worked in three teams, and each team consisted of three to four experts and graduate students. The collected data for inspected structures includes damage levels, structural and/or architectural drawings, dimensions, global positioning system coordinates, and photographs.

In the survey, damaged structures were classified into three damage categories: light, moderate, and severe damage states (Sim *et al*. 2018). Fig. 10 displays some photos of actual damaged buildings for three damage states collected from post-earthquake survey.

The reconnaissance teams originally focused on the inspection of various types of damaged building structures including piloti-type buildings. To obtain more accurate fragility estimates for four-story piloti-type RC buildings in the target area, an additional on-site survey was performed for eight days in January 2019 by the Structural Reliability and Disaster Risk research group of Ulsan National Institute of Science and Technology (UNIST). The on-site survey data includes building address, number of stories, and photographs of all selected piloti-type buildings in the target area. Additionally, detailed building information such as building use, height, floor area, and structural type was collected from the database operated by the Ministry of Land, Infrastructure and Transport in Korea which is open to the public through the website of Electronic Architectural administration Information System (E-AIS). Based on the comprehensive data collected from reconnaissance, on-site survey, and E-AIS database, empirical failure probabilities were estimated for the damage states considered in this study. A total of 538 four-story piloti-type RC buildings were considered in this example, and Fig. 11 reveals their locations. Among them, damaged buildings were marked with different colors, such as blue (for light damage), black (for moderate damage), and red (for severe damage). A total of 18, 9, and 25 buildings were identified as lightly, moderately, and severely damaged, respectively, and Table 6 gives empirical failure probabilities for the three damage

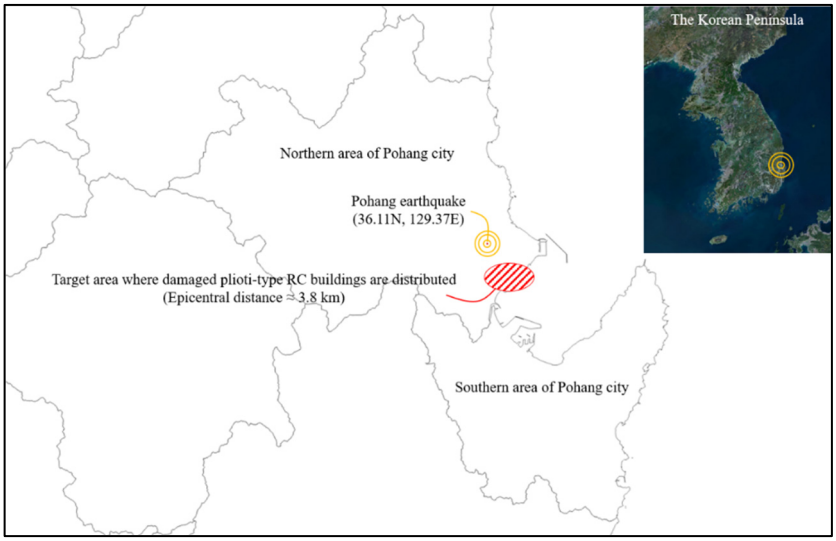

Fig. 9 Location of the occurrence of the Pohang earthquake epicenter and the target area

(a) Light damage

(b) Moderate damage

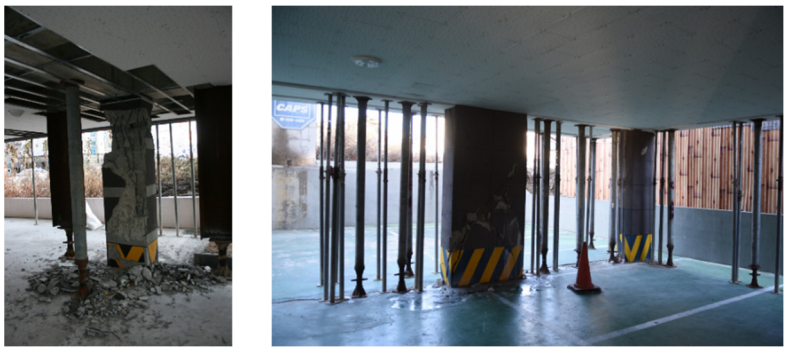

(c) Severe damage

Fig. 10 Pictures of damaged buildings (Sim *et al*. 2018)

states. It is noteworthy that the failure probabilities in the table are cumulative probabilities according to the definition of seismic fragility curves.

3.5 Derivation of hybrid fragility curves

After evaluating empirical failure probabilities (presented in Table 6), the c.o.v.s of capacity thresholds for the damage limit states were updated, being optimized to the empirical failure probabilities. An optimization algorithm in MATLAB was linked to the FERUM-ZEUS, whose flowchart can be found in Fig. 3. The c.o.v.s were considered as the likelihood of the c.o.v. being observed in the target area, and the initially assumed (prior) c.o.v.s were revised via Bayesian updating, as given in Eq. (2). The updated (posterior) c.o.v.s were then applied to derive hybrid fragility curves. Table 7 shows the variations in the prior, likelihood, and posterior c.o.v.s for the three damage limit states. The prior c.o.v.s of capacity thresholds were

Table 6 Empirical failure probabilities for three damage states

Damage state	Empirical failure probability
Light	0.0967
Moderate	0.0632
Severe	0.0465

Table 7 Variations in the prior, likelihood, and posterior c.o.v. values for each damage state

Damage state	Prior	Likelihood	Posterior
Light	0.307	0.233	0.265
Moderate	0.307	0.379	0.338
Severe	0.307	0.433	0.362

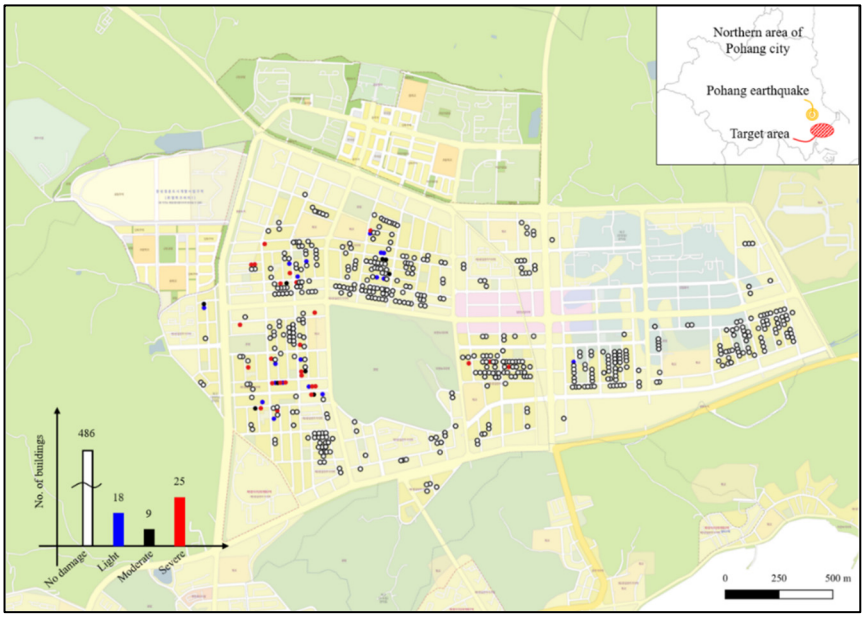

Fig. 11 Locations of piloti-type RC buildings in the target area

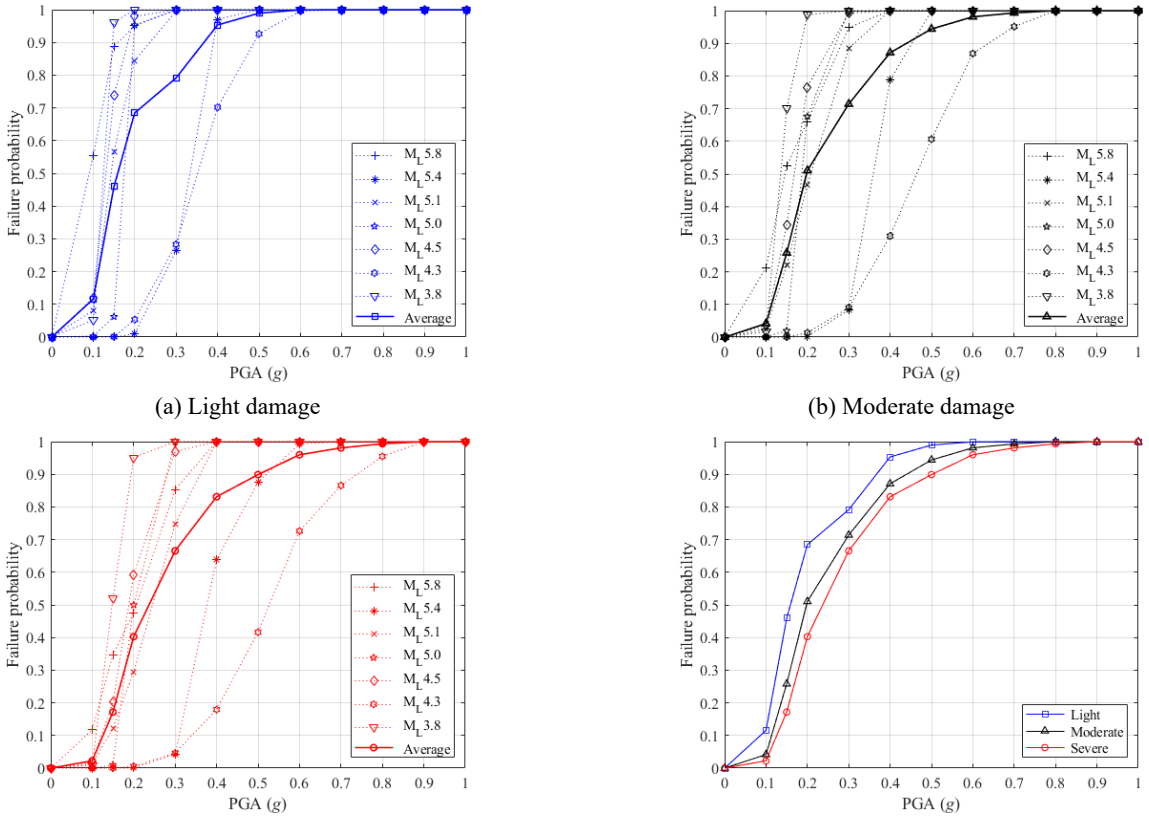

(a) Light damage

(b) Moderate damage

(c) Severe damage

(d) Average fragility curves

Fig. 12 Hybrid fragility curves

assumed to be 0.307 for all limit states. However, the posterior c.o.v.s, updated to reflect the empirical damage likelihood, were changed to 0.265 (for light damage), 0.338 (for moderate), and 0.362 (for severe damage), and it was found that the posterior c.o.v. increased as the damage level increased. The posterior c.o.v. variation trend, which depends on the damage state, consistently conformed to the finding of previous studies that the level of capacity uncertainty tends to increase as the damage level increases (Yu *et al*. 2016, Dolšek 2012).

Using the posterior c.o.v.s with the FERUM-ZEUS platform, fragility analysis was performed again to draw

Table 8 Average failure probabilities of the hybrid fragility curves for each damage state

Damage state	PGA (g)										
	0.1	0.15	0.2	0.3	0.4	0.5	0.6	0.7	0.8	0.9	1.0
Light	0.116	0.459	0.684	0.792	0.953	0.990	0.999	1	1	1	1
Moderate	0.042	0.258	0.510	0.714	0.871	0.944	0.981	0.993	1	1	1
Severe	0.022	0.172	0.403	0.666	0.831	0.899	0.960	0.981	0.994	1	1

Table 9 Comparison of the analytical, hybrid, and empirical failure probabilities at 0.27 g PGA

Damage state	Analytical failure probability	Hybrid failure probability	Empirical failure probability
Light	0.1774	0.1342	0.0967
Moderate	0.0235	0.0405	0.0632
Severe	0.0055	0.0204	0.0465

hybrid seismic fragility curves. Fig. 12 demonstrates the updated fragility curves for the three damage states. As done for analytical fragility assessment, hybrid fragility curves were plotted for all selected earthquake motions and the average fragility curves were presented at the same time. Table 8 offers the average failure probabilities of the hybrid fragility curves with varying ground motion intensities. When the 2017 Pohang earthquake occurred, the PGA of the actual ground motion in the target area was estimated to be approximately 0.27 g (Kim *et al*. 2020b). Table 9 reveals the analytical, hybrid, and empirical failure probabilities at the PGA of 0.27 g, and it is observed that the hybrid fragility estimates were updated closer to the empirical probabilities than the analytical fragility estimates. This implies that the updated (posterior) c.o.v.s of the capacity threshold better reflect the empirical failure likelihoods of the structure in the target area.

4. Verification of the proposed method

4.1 Problem description with hypothetical reconnaissance data sets

In the previous illustration example, seismic fragility curves were updated once because only one set of empirical data was available in the target area, as presented in Table 6. However, if sufficient empirical datasets are gathered from the same area, the c.o.v. of the capacity threshold can be updated further and is expected to converge to the true value. To verify this, series of c.o.v. updates were conducted exploring hypothetical reconnaissance data sets created based on assumed c.o.v.s.

To determine the true c.o.v.s of capacity thresholds for the target piloti-type structure, 1,000 samples were generated considering the same random variables and their statistical properties presented in Table 3. Then, nonlinear pushover analyses were performed using the 1000 sample models using ZEUS-NL, and the c.o.v. values were estimated to be 0.1099 (for light damage), 0.1494 (for moderate damage), and 0.3026 (for severe damage). Fig. 13 demonstrates the nonlinear pushover curves of the 1,000 analytical models.

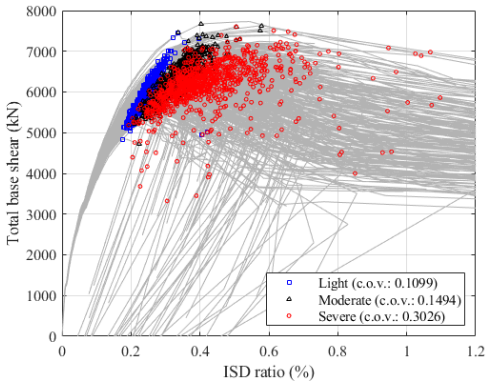

Fig. 13 Nonlinear pushover curves for 1,000 sample sets

Failure probabilities were computed with the true c.o.v.s using FERUM-ZEUS. Based on the computed failure probabilities, the hypothetical empirical fragilities were generated after assigning some degree of errors to the failure probabilities to mimic the judgmental errors that might arise from post-earthquake reconnaissance. For comparison, 10% and 1% errors were assigned separately. With each level of errors, seven sets of artificial reconnaissance data were generated about various input ground motions and PGAs.

4.2 Analysis results and discussions

By making use of the artificially-generated failure probabilities, an optimization analysis (in Fig. 3) was performed with each input ground motion and for each damage state to obtain the c.o.v.s corresponding to the hypothetical failure probabilities. Table 10 presents the the c.o.v.s obtained from the optimization analyses based on the artificial reconnaissance data.

Finally, the c.o.v.s were updated sequentially through Bayesian updating, where the prior c.o.v.s of 0.307 were employed as in the illustrative example. Table 11 gives Bayesian updating results using the artificial c.o.v.s with 10% and 1% errors; Fig. 14 shows the difference between the updated c.o.v.s (in Table 11) and true c.o.v.s (i.e., 0.1099 for light damage, 0.1494 for moderate damage, and 0.3026 for severe damage). For the light damage state, the results show that the c.o.v. consistently converges to the true c.o.v. as the updating continues in both cases of 10% and 1% errors. For the moderate damage state, the results accurately verify the decreasing trend as the number of updates

Table 10 The c.o.v. values obtained based on artificial reconnaissance data

Damage state	Error	M_L3.8 (0.14 *g* PGA)	M_L5.0 (0.19 *g* PGA)	M_L5.1 (0.20 *g* PGA)	M_L5.8 (0.14 *g* PGA)	M_L4.5 (0.18 *g* PGA)	M_L5.4 (0.36 *g* PGA)	M_L4.3 (0.48 *g* PGA)
Light	10%	0.1331	0.1118	0.1444	0.1387	0.1444	0.1537	0.1297
	1%	0.1061	0.1118	0.1186	0.1176	0.1354	0.1427	0.1264
Moderate	10%	0.1618	0.1764	0.1764	0.1944	0.1056	0.1852	0.1964
	1%	0.1236	0.1764	0.1416	0.1504	0.1315	0.1397	0.1382
Severe	10%	0.2646	0.2882	0.2646	0.2849	0.2703	0.2837	0.2736
	1%	0.2736	0.2736	0.2971	0.3001	0.2846	0.2988	0.3028

Table 11 Results of Bayesian updating on the artificial c.o.v.s

Damage state	Error	0 (prior)	1	2	3	4	5	6
Light	10%	0.307	0.2006	0.1643	0.1585	0.1538	0.1519	0.1518
	1%	0.307	0.1791	0.1523	0.1426	0.1368	0.1362	0.1368
Moderate	10%	0.307	0.2212	0.2041	0.1961	0.1952	0.1757	0.1767
	1%	0.307	0.1933	0.1866	0.1735	0.1681	0.1610	0.1574
Severe	10%	0.307	0.2829	0.2832	0.2774	0.2781	0.2761	0.2766
	1%	0.307	0.2877	0.2815	0.2843	0.2865	0.2855	0.2867

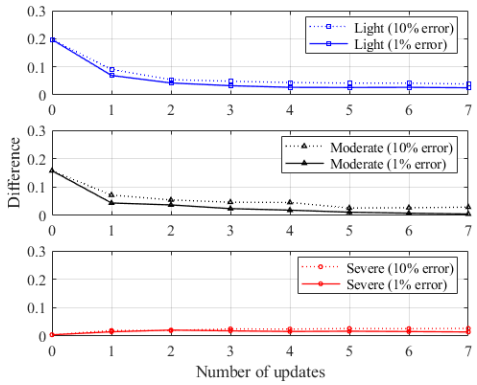

Fig. 14 Difference between the updated c.o.v. and true c.o.v.

increases for both error cases. In particular, the c.o.v. converges to the true c.o.v. very quickly for the case of 1% error. For the severe damage state, the difference between the prior c.o.v. (i.e., 0.307) and true c.o.v. (i.e., 0.3026) was small from the beginning of the update, and the small difference continues. The 1% error case shows better convergence than the 10% error case for all damage states. That is, if careful damage inspection is conducted during post-earthquake survey, the c.o.v. of the capacity threshold is expected to converge to the specific value after few updating as desired by the hybrid method. The logic of the proposed hybrid method was fully verified through a series of updates using the artificial reconnaissance data. From this analysis results, it was confirmed that the proposed method could provide more reliable and accurate fragility curves if sufficient empirical data is accessible in a target area.

5. Conclusions

This study proposed a new hybrid method to derive fragility curves using post-earthquake reconnaissance data and numerical analysis results from an FE model. For cost-efficient fragility assessment and optimization, this study introduces a computational platform of FERUM-ZEUS. The proposed method consists of four steps, which are 1) the derivation of analytical fragility curves; 2) the identification of probabilistic distribution parameters of capacity thresholds through optimization; 3) the updates of the distribution parameters using the Bayesian updating; and 4) the derivation of hybrid fragility curves with the updated distribution parameters.

To illustrate the proposed method, it was applied to an example of an actual earthquake event (i.e., 2017 Pohang earthquake). Analytical fragility curves were first derived based on the FE model constructed to represent piloti-type RC buildings in the damaged area with the assumed (prior) c.o.v.s of capacity thresholds. After the prior c.o.v.s were updated based on the empirical failure probabilities estimated from post-earthquake reconnaissance data, the updated (posterior) c.o.v.s that best describe the empirical failure probabilities were used to develop the hybrid fragility curves. The results showed that the seismic fragility estimates approached to the empirical failure probabilities at 0.27 *g* PGA, corresponding to the ground motion intensity of the Pohang earthquake.

In addition, it was confirmed that the proposed method could provide more realistic fragility curves as well as converged distribution parameters of capacity thresholds, if empirical data is sufficient. In the verification example, seven artificial sets of reconnaissance data were generated, and errors of 10% and 1% were assigned to the failure probabilities obtained using the true c.o.v. The artificial

c.o.v.s were updated sequentially, and it was identified that the c.o.v.s accurately converged to the true c.o.v.s. It was also found that the case of 1% error had better convergence than that of 10% error, which means the accuracy of seismic fragility assessment would increase with better reconnaissance data. The analysis results show that the proposed hybrid method could provide more robust and accurate fragility curves when enough empirical data is provided in a target area.

Acknowledgments

This research was supported by a grant (2020-MOIS31-013) of Fundamental Technology Development Program for Extreme Disaster Response funded by Ministry of Interior and Safety (MOIS, Korea).

References

Ang, A.H.-S. and Tang, W.H. (2007), *Probability Concepts in Engineering*: *Emphasis on Applications to Civil and Environmental Engineering*, (2nd Edition), John Wiley & Sons, Hoboken, NJ, USA.

Askan, A. and Yucemen, M.S. (2010), "Probabilistic methods for the estimation of potential seismic damage: Application to reinforced concrete buildings in Turkey", *Struct. Saf.*, **32**(4), 262-271. https://doi.org/10.1016/j.strusafe.2010.04.001

Barbato, M., Gu, Q. and Conte, J.P. (2010), "Probabilistic push-over analysis of structural and soil-structure systems", *J. Struct. Eng.*, **136**(11), 1330-1341. https://doi.org/10.1061/(ASCE)ST.1943-541X.0000231

Der Kiureghian, A. (2005), *First- and Second-Order Reliability Methods*, *Engineering Design Reliability Handbook*, (edited by Nikolaidis, E., Ghiocel, D.M. and Singhal, S.), Chapter 14, CRC Press, Boca Raton, FL, USA.

Dolšek, M. (2012), "Simplified method for seismic risk assessment of buildings with consideration of aleatory and epistemic uncertainty", *Struct. Infrastruct. Eng.*, **8**(10), 939-953. https://doi.org/10.1080/15732479.2011.574813

Ellingwood, B.R., Celik, O.C. and Kinali, K. (2007), "Fragility assessment of building structural systems in Mid-America", *Earthq. Eng. Struct. Dyn.*, **36**(13), 1935-1952. https://doi.org/10.1002/eqe.693

Elnashai, A.S., Papanikolaou, V.K. and Lee, D. (2010), "ZEUS NL - A System for Inelastic Analysis of Structures", User's manual; Mid-America Earthquake (MAE) Center, Department of Civil and Environmental Engineering, University of Illinois at Urbana-Champaign, Urbana, IL, USA.

Federal Emergency Management Agency (FEMA) (2013), "Hazus—MH 2.1: Technical manual. Multi-hazard loss estimation methodology, earthquake model".

Giordano, N., De Luca, F., Sextos, A., Cortes, F.R., Ferreira, C.F. and Wu, J. (2021), "Empirical seismic fragility models for Nepalese school buildings", *Nat. Hazards*, **105**, 339-362. https://doi.org/10.1007/s11069-020-04312-1

Güneyisi, E.M. and Altay, G. (2008), "Seismic fragility assessment of effectiveness of viscous dampers in R/C buildings under scenario earthquakes", *Struct. Saf.*, **30**(5), 461-480. https://doi.org/10.1016/j.strusafe.2007.06.001

Haukaas, T. (2003), "Finite element reliability and sensitivity methods for performance-based engineering", Ph.D. Dissertation; University of California, Berkeley, CA, USA.

Hueste, M.B.D. and Bai, J.W. (2007), "Seismic retrofit of a reinforced concrete flat-slab structure: Part II—Seismic fragility analysis", *Eng. Struct.*, **29**(6), 1178-1188. https://doi.org/10.1016/j.engstruct.2006.07.022

Jaiswal, K.S., Aspinall, W., Perkins, D., Wald, D. and Porter, K.A. (2012), "Use of expert judgment elicitation to estimate seismic vulnerability of selected building types", *Proceedings of the 15th World Conference on Earthquake Engineering*, Lisbon, Portugal, September.

Ji, J., Elnashai, A.S. and Kuchma, D.A. (2009), "Seismic fragility relationships of reinforced concrete high-rise buildings", *Struct. Des. Tall Spec.*, **18**(3), 259-277. https://doi.org/10.1002/tal.408

Kang, S., Kim, B., Bae, S., Lee, H. and Kim, M. (2019), "Earthquake-induced ground deformations in the low-seismicity region: a case of the 2017 M5.4 Pohang, South Korea, earthquake", *Earthq. Spectra*, **35**, 1235-1260. https://doi.org/10.1193/062318EQS160M

Kappos, A.J., Stylianidis, K.C. and Pitilakis, K. (1998), "Development of seismic risk scenarios based on a hybrid method of vulnerability assessment", *Nat. Hazards*, **17**(2), 177-192, https://doi.org/10.1023/A:1008083021022

Kappos, A.J., Panagopoulos, G., Panagiotopoulos, C. and Penelis, G. (2006), "A hybrid method for the vulnerability assessment of R/C and URM buildings", *B. Earthq. Eng.*, **4**(4), 391-413. https://doi.org/10.1007/s10518-006-9023-0

Kim, H., Sim, S.-H., Lee, J., Lee, Y.-J. and Kim, J.-M. (2017), "Flood fragility analysis for bridges with multiple failure modes", *Adv. Mech. Eng.*, **9**(3), 1-11. https://doi.org/10.1177/1687814017696415

Kim, T., Chu, Y., Kim, S.R. and Bhandari, D. (2018), "Seismic behavior of domestic piloti-type buildings damaged by 2017 Pohang earthquake", *J. Earthq. Eng. Soc. Korea*, **22**(3), 161-168, (in Korean), https://doi.org/10.5000/EESK.2018.22.3.161

Kim, B., Ji, Y., Kim, M., Lee, Y.-J., Kang, H., Yun, N.-R., Kim, H. and Lee, J. (2020a), "Building damage caused by the 2017 M5.4 Pohang, South Korea, earthquake, and effects of ground conditions", *J. Earthq. Eng.*, 1-19. https://doi.org/10.1080/13632469.2020.1785585

Kim, H.-S., Kim, M., Baise, L.G. and Kim, B. (2020b), "Local and regional evaluation of liquefaction potential index and liquefaction severity number for liquefaction-induced sand boils in Pohang, South Korea", *Soil Dyn. Earthq. Eng.*, 106459. https://doi.org/10.1016/j.soildyn.2020.106459

Kircher, C.A., Whitman, R.V. and Holmes, W.T. (2006), "HAZUS earthquake loss estimation methods", *Nat. Hazards Rev.*, **7**(2), 45-59. https://doi.org/10.1061/(ASCE)1527-6988(2006)7:2(45)

Kwon, O.-S. and Elnashai, A. (2006), "The effect of material and ground motion uncertainty on the seismic vulnerability curves of RC structure", *Eng. Struct.*, **28**(2), 289-303. https://doi.org/10.1016/j.engstruct.2005.07.010

Lee, Y.-J. and Moon, D.-S. (2014), "A new methodology of the development of seismic fragility curves", *Smart Struct. Syst., Int. J.*, **14**(5), 847-867. http://dx.doi.org/10.12989/sss.2014.14.5.847

Lee, Y.-J. and Song, J. (2012), "Finite-element-based system reliability analysis of fatigue-induced sequential failures", *Reliab. Eng. Syst. Safe.*, **108**, 131-141. https://doi.org/10.1016/j.ress.2012.05.007

Lee, Y.-J., Song, J. and Tuegel, E. (2008), "Finite element system reliability analysis of a wing torque box", *Proceedings of the 10th AIAA Nondeterministic Approaches Conference*, Schaumburg, IL, USA, April.

Lee, J., Lee, Y.-J., Kim, H., Sim, S.-H. and Kim, J.-M. (2016), "A new methodology development for flood fragility curve derivation considering structural deterioration for bridges", *Smart Struct. Syst., Int. J.*, **17**(1), 149-165. http://dx.doi.org/10.12989/sss.2016.17.1.149

Li, L.-X., Li, H.-N. and Li, C. (2018), "Seismic fragility

assessment of self-centering RC frame structures considering maximum and residual deformations", *Struct. Eng. Mech., Int. J.*, **68**(6), 677-689. https://doi.org/10.12989/sem.2018.68.6.677

Liu, Z. and Zhang, Z. (2017), "Fragility analysis of concrete-filled steel tube arch bridge subjected to near-fault ground motion considering the wave passage effect", *Smart Struct. Syst., Int. J.*, **19**(4), 415-429. https://doi.org/10.12989/sss.2017.19.4.415

Martínez, A., Hube, M.A. and Rollins, K.M. (2017), "Analytical fragility curves for non-skewed highway bridges in Chile", *Eng. Struct.*, **141**, 530-542. https://doi.org/10.1016/j.engstruct.2017.03.041

Montiel, M.A. and Ruiz, S.E. (2007), "Influence of structural capacity uncertainty on seismic reliability of buildings under narrow-band motions", *Earthq. Eng. Struct. Dyn.*, **36**(13), 1915-1934. https://doi.org/10.1002/eqe.711

Moon, D.-S., Lee, Y.-J. and Lee, S. (2018), "Fragility analysis of space reinforced concrete frame structures with structural irregularity in plan", *J. Struct. Eng.*, **144**(8), 04018096. https://doi.org/10.1061/(ASCE)ST.1943-541X.0002092

Moradloo, J., Naserasadi, K. and Zamani, H. (2018), "Seismic fragility evaluation of arch concrete dams through nonlinear incremental analysis using smeared crack model", *Struct. Eng. Mech., Int. J.*, **68**(6), 747-760. https://doi.org/10.12989/sem.2018.68.6.747

Mosleh, A. and Apostolakis, G. (1986), "The assessment of probability distributions from expert opinions with an application to seismic fragility curves", *Risk Anal.*, **6**(4), 447-461. https://doi.org/10.1111/j.1539-6924.1986.tb00957.x

Paik, I.-Y., Shim, C.-S., Chung, Y.-S. and Sang, H.-J. (2011), "Statistical properties of material strength of concrete, re-bar and strand used in domestic construction site", *J. Korea Concr. Inst.*, **23**(4), 421-430. [In Korean] https://doi.org/10.4334/JKCI.2011.23.4.421

Park, Y.-J. and Ang, A.H.-S. (1985), "Mechanistic seismic damage model for reinforced concrete", *J. Struct. Eng.*, **111**(4), 722-739. https://doi.org/10.1061/(ASCE)0733-9445(1985)111:4(722)

Pitilakis, K., Crowley, H. and Kaynia, A.M. (2014), "SYNER-G: typology definition and fragility functions for physical elements at seismic risk", *Geotec. Geol. Earthq. Eng.*, **27**, 1-28. https://doi.org/10.1007/978-94-007-7872-6

Ramamoorthy, S.K., Gardoni, P. and Bracci, J.M. (2006), "Probabilistic demand models and fragility curves for reinforced concrete frames", *J. Struct. Eng.*, **132**(10), 1563-1572. https://doi.org/10.1061/(ASCE)0733-9445(2006)132:10(1563)

Razzaghi, M.S., Safarkhanlou, M., Mosleh, A. and Hosseini, P. (2018), "Fragility assessment of RC bridges using numerical analysis and artificial neural networks", *Earthq. Struct., Int. J.*, **15**(4), 431-441. http://dx.doi.org/10.12989/eas.2018.15.4.431

Rossetto, T. and Elnashai, A. (2003), "Derivation of vulnerability functions for European-type RC structures based on observational data", *Eng. Struct.*, **7**(3), 1241-1263. https://doi.org/10.1016/S0141-0296(03)00060-9

Rosti, A., Rota, M. and Penna, A. (2020), "Empirical fragility curves for Italian URM buildings", *Bull. Earthq. Eng.*, **19**(8), 3057-3076. https://doi.org/10.1007/s10518-020-00845-9

Silva, V., Crowley, H., Varum, H., Pinho, R. and Sousa, R. (2014), "Evaluation of analytical methodologies used to derive vulnerability functions", *Earthq. Eng. Struct. Dyn.*, **43**(2), 181-204. https://doi.org/10.1002/eqe.2337

Sim, C., Laughery, L., Chiou, T.C. and Weng, P.-W. (2018), 2017 Pohang Earthquake - Reinforced Concrete Building Damage Survey. https://datacenterhub.org/resources/14728

Singhal, A. and Kiremidjian, A.S. (1998), "Bayesian updating of fragilities with application to RC frames", *J. Struct. Eng.*, **124**(8), 922-929. https://doi.org/10.1061/(ASCE)0733-9445(1998)124:8(922)

Steelman, J., Song, J. and Hajjar, J.F. (2007), "Integrated data flow and risk aggregation for consequence-based risk management of seismic regional loss", Mid-America Earthquake Center, University of Illinois at Urbana-Champaign, Urbana, IL, USA, November.

Vamvatsikos, D. and Cornell, C.A. (2002), "Incremental dynamic analysis", *Earthq. Eng. Struct. Dyn.*, **31**(3), 491-514. https://doi.org/10.1002/eqe.141

Wen, Y.K., Ellingwood, B.R. and Bracci, J.M. (2004), "Vulnerability function framework for consequence-based engineering", MAE Center Report 04-04.

Yoon, S., Lee, Y.-J. and Jung, H.-J. (2018), "A comprehensive framework for seismic risk assessment of urban water transmission", *Int. J. Disast. Risk Re.*, **31**, 983-994. https://doi.org/10.1016/j.ijdrr.2018.09.002

Yu, X., Lu, D. and Li, B. (2016), "Estimating uncertainty in limit state capacities for reinforced concrete frame structures through pushover analysis", *Earthq. Struct., Int. J.*, **10**(1), 141-161. https://doi.org/10.12989/eas.2016.10.1.141

HJ